ELSEVIER

Journal of Photochemistry and Photobiology A: Chemistry 154 (2002) 53–60

Journal of Photochemistry and Photobiology A:Chemistry

www.elsevier.com/locate/jphotochem

Excited-state proton transfer to solvent of protonated aniline derivatives in aqueous solution: a remarkable effect of *ortho* alkyl group on the proton-dissociation rate

Satoru Shiobara, Rie Kamiyama, So Tajima, Haruo Shizuka, Seiji Tobita*

Department of Chemistry, Gunma University, Kiryu, Gunma 376-8515, Japan

Received 10 April 2002; received in revised form 14 June 2002; accepted 14 June 2002

Abstract

Proton dissociation from the lowest excited singlet state of protonated aniline (AN) derivatives in aqueous solution has been studied by picosecond time-resolved fluorescence measurements. The proton-dissociation rate is significantly influenced by introduction of *ortho* alkyl group(s) to AN as 1.4×10^{10} s^{-1} for AN, 4.1×10^{9} s^{-1} for 2-toluidine and 1.7×10^{9} s^{-1} for 2,6-xylidine. The remarkable decrease of the proton-dissociation rate by alkylation is attributed partly to change in exothermicity of the reactions. The activation barrier for the proton-dissociation reaction is increased in the alkylated ANs, suggesting that the hydrophobic effects of the alkyl group on the water structure in the vicinity of the amino group influences the rate of proton transfer to solvent.

Keywords: Proton transfer; Fluorescence; Quenching; Substituent effect; Aniline; Hydrophobic effect

1. Introduction

Proton transfer has been extensively investigated as one of the most fundamental processes in chemistry [1–8]. They include intramolecular proton transfer of aromatic compounds in the excited state, excited-state intermolecular proton transfer in a hydrogen-bonded complex, and also excited-state proton transfer of various photoacids to solvent. In the last case, solvent molecule(s) acts as proton acceptor and, therefore, the solvent plays a crucial role in the reaction.

Recent development of ultrafast spectroscopy has enabled us to measure directly the proton-dissociation rate of various types of photoacids with sufficiently high time resolution [3]. Among them, hydroxyarenes (ROH) [9–33] and aromatic amines (RNH_2) [34–40] have been most extensively studied because of their remarkable changes in acidity upon electronic excitation. In the hydroxyarenes the excited-state proton dissociation is usually followed by a geminate recombination process. Since the geminate recombination occurs adiabatically, the fluorescence time profile of ROH^* exhibits a nonexponential decay. Agmon et al. [18,19,41] applied the theory of geminate diffusion-influenced reactions to the excited-state proton transfer to solvent of hydroxyarenes according to the following two-step model:

$$ROH^* \underset{k_{rec}}{\overset{k_{dis}}{\rightleftharpoons}} [RO^{-*} \cdots H^+]_{r=a} \overset{DSE}{\rightleftharpoons} RO^{-*} + H^+ \quad (1)$$

The first chemical step is described by the back-reaction boundary condition with intrinsic rate constants k_{dis} and k_{rec} and is followed by diffusional step in which the hydrated proton is separated from the contact radius, a, to infinity. The second step is described by the exact transient (numerical) solution of the Debye–Smoluchowski equation (DSE) with the above mentioned boundary condition. In the above reactions (Eq. (1)) Coulombic interactions in the geminate ion-pair play an important role in the occurrence of the geminate recombination.

In aromatic amines, on the other hand, precursor molecules of proton transfer reactions are protonated amines. Hence, the proton transfer to solvent produces an excited amine ($RNH_2{}^*$) and a proton. Since the Coulombic interactions in the geminate product pair, $[RNH_2{}^* \cdots H^+]$, are negligible, the proton-dissociation rate can be determined more accurately from analysis of the exponential decay of $RNH_3{}^{+*}$ or the rise and decay profile of $RNH_2{}^*$.

Fleming et al. studied excited-state proton transfer of protonated 1-aminopyrene in water–organic solvent mixtures [38] and in inclusion complexes with β-cyclodextrin [39]. In contrast to the similar measurements on ROH type

* Corresponding author. Tel.: +81-277-30-1210; fax: +81-277-30-1213.
E-mail address: tobita@chem.gunma-u.ac.jp (S. Tobita).

1010-6030/02/$ – see front matter © 2002 Elsevier Science B.V. All rights reserved.
PII: S1010-6030(02)00310-6

photoacids, the proton-dissociation rate increased in all water–organic solvent mixtures up to 60–75% of the organic solvent. They showed that the photoacid dissociation rates followed a general structure–reactivity law which correlates the proton-dissociation rate with the pK_a values of the precursor acid. For the inclusion complexes with β-cyclodextrin they suggested that the water near the cavity rim of β-cyclodextrin was modified by the extensive network on OH groups in such a way as to increase its basicity.

Proton dissociation and acid–base equilibrium in the excited state are also affected by substituent introduced in the aromatic ring [42–44]. Schulman et al. [43] determined the rate constants for prototropic dissociation and reprotonation in the lowest excited singlet state (S_1) of the three isomeric cyanophenols by fluorimetric titrimetry. They found that in the S_1 state the *ortho* isomer was the strongest acid and the *para* isomer the weakest. The results were rationalized qualitatively in terms of the degree of coupling of the $^1L_b \rightarrow {}^1A$ transition moment with the moment corresponding to the direction of electronic interactions of the substituents with the benzene ring in each isomer. Tolbert and Huppert [23–26] reported a remarkably increased photoacidity of 5-cyano-1-naphthol and 5,8-dicyano-1-naphthol, which was explained based on the charge migration from the hydroxyl group to C-5 and C-8 positions in the S_1 state.

In the present work, we studied the proton dissociation of aniline (AN) and its *ortho* alkylated compounds by using a femtosecond laser combined with a time-correlated single-photon counting system. Scheme 1 shows proton dissociation and association reactions of aqueous AN derivatives in the ground and excited singlet states. The proton dissociation of protonated AN (ANH^+) was found to occur within about 70 ps, which was the fastest among protonated amines investigated so far. The proton-dissociation rate in the S_1 state decreased remarkably by *ortho* substitution, in spite of the relatively weak electronic effect of the alkyl group. The influence of the *ortho* alkyl group on the proton-dissociation rate is ascribed to modified water structure and mobility around the amino group.

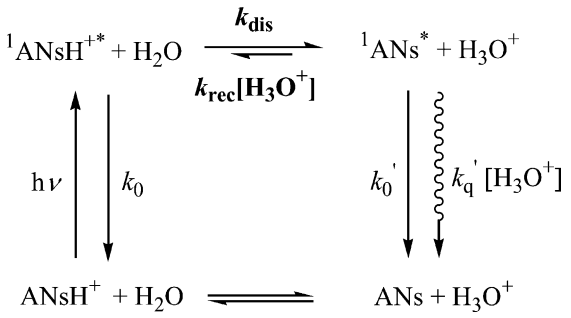

Scheme 1. Kinetic scheme for prototropism of $ANsH^+$ in aqueous solution.

2. Experimental

AN (Kanto), 4-toluidine (4-TL, Tokyo kasei), 2-toluidine (2-TL, Tokyo kasei), 2-ethylaniline (2-EAN, Tokyo kasei), 2,6-xylidine (2,6-XY, Kanto), and 2,6-diethylaniline (2,6-DEAN, Tokyo kasei) (see Scheme 2) and *N*,*N*-dimethylaniline (DMA, Wako) were purified by vacuum distillation. *N*,*N*-Dimethyl-2,6-xylidine (DMXY) was made by methylation of 2,6-XY with trimethyl phosphate. The product, DMXY, was purified by column chromatography on silica gel and then distilled under reduced pressure. Cyclohexane (CH, Aldrich, spectrophotometric grade) was used as received. Acetonitrile (MeCN, Kanto) was purified by distillation. Deionized water was purified by using a Millipore (MILLI-Q-Labo). H_2SO_4 (Wako, 97% pure, S.S. grade) was used as received. The pH values of sample solutions were determined by a pH meter (Horiba, F-8). Sample concentrations were 10^{-4}–5×10^{-3} M. All sample solutions for fluorescence measurements were saturated with argon gas or degassed by freeze–pump–thaw cycles on a high-vacuum line prior to experiments.

The absorption and fluorescence spectra were measured with an UV/Vis spectrophotometer (Jasco, Ubest-50) and a spectrofluorometer (Hitachi, F-4010), respectively. Nanosecond time-resolved fluorescence measurements were carried out by using a time-correlated single-photon counting fluorometer (Edinburgh Analytical Instruments, FL-900-CDT). A nanosecond pulsed discharge lamp (pulse width: ~1.0 ns, repetition rate: 40 kHz) filled with hydrogen gas was used as the excitation light source. Picosecond time-resolved fluorescence measurements were made by using a femtosecond-laser system which was based on a mode-locked Ti:sapphire laser (Spectra-Physics, Tsunami; 800 nm,

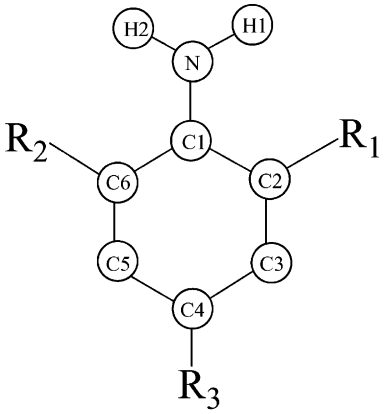

R_1=H, R_2=H, R_3=H : Aniline **(AN)**
R_1=H, R_2=H, R_3=CH_3 : 4-Toluidine **(4-TL)**
R_1= CH_3, R_2=H, R_3= H : 2-Toluidine **(2-TL)**
R_1= C_2H_5, R_2=H, R_3=H : 2-Ethylaniline **(2-EAN)**
R_1=CH_3, R_2= CH_3, R_3=H : 2,6-Xylidine **(2,6-XY)**
R_1=C_2H_5, R_2= C_2H_5, R_3=H: 2,6-Diethylaniline **(2,6-DEAN)**

Scheme 2. Molecular structures of ANs.

FWHM ∼70 fs, at 80 MHz) pumped by a CW green laser (Spectra-Physics, Millennia V; 532 nm, 4.5 W) [45]. The repetition rate was adjusted to 4 MHz by using a pulse-picker (Spectra-Physics, Model 3980), and the third harmonic (266 nm, FWHM ∼250 fs) was used for the excitation source. The monitoring system consisted of a microchannel-plate photomultiplier tube (MCP-PMT; Hamamatsu, R380-9U-51) cooled at −20 °C and a single-photon counting module (Becker and Hickl, SPC-530). The fluorescence photon signal detected by the MCP-PMT and the photon signal of the second harmonic (400 nm) of the Ti:sapphire laser were used for the start and stop pulses of time-to-amplitude converter in this system. The instrumental response function had a half-width of about 20 ps. The fluorescence time profiles were analyzed by iterative reconvolution with the response function. In temperature effect experiments the temperature of each sample solution was controlled by a constant temperature circulator (IWAKI, CLU-S21).

Molecular orbital (MO) calculations were performed by use of the ab initio MO method (Gaussian 98) on a personal computer [46]. The molecular geometries of AN and 2,6-XY in the ground state were optimized at B3LYP/6-31G* level.

3. Results and discussion

3.1. Absorption and fluorescence spectra

In Fig. 1 the absorption and fluorescence spectra of DMA, DMXY, AN, and 2,6-XY in CH and acetonitrile at 298 K are shown to inspect the steric effect of the *o*-dimethyl groups on the conformation of the amino group. It is noted that the first absorption band of DMXY is significantly blue-shifted compared to that of DMA (Fig. 1(a) and (b)). This clearly indicates that the dimethyl amino group in DMXY is strongly twisted with respect to the phenyl moiety, decreasing the electronic conjugation between the amino lone-pair and the aromatic π–electron system. In contrast with the absorption spectra, the fluorescence spectrum of DMXY is red-shifted compared with that of DMA, resulting in a very large Stokes shift for DMXY ($\Delta\nu_f = 9100\,cm^{-1}$) even in nonpolar CH. This large Stokes shift in nonpolar solvent manifests a structural change of the amino group from twisted to more planar conformation upon electronic excitation [47–50].

The first absorption band of 2,6-XY, on the other hand, is only slightly blue-shifted compared with that of AN (Fig. 1(c) and (d)), suggesting almost the same twist angle and conformation of the amino group in AN and 2,6-XY. The MO calculations (B3LYP/6-31G*) on the optimized geometries of AN and 2,6-XY also gave similar geometries for AN and 2,6-XY; the dihedral angles, C2–C1–N–H1 and C6–C1–N–H2, for AN were 26.525 and −26.543, those for 2,6-XY were 26.455 and –26.515, respectively, and the H1–N–H2 angles for AN and 2,6-XY were 110.927 and 110.876, respectively (see Scheme 2).

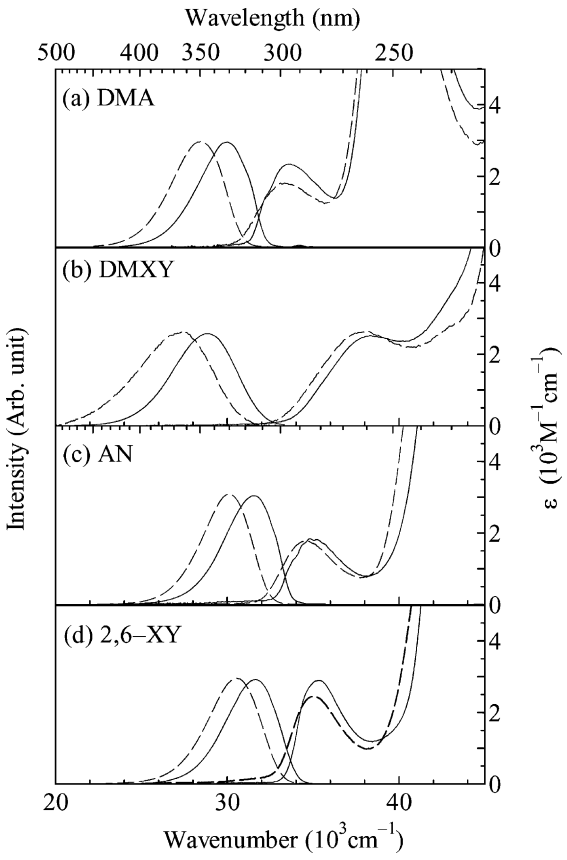

Fig. 1. Absorption and fluorescence spectra of (a) DMA, (b) DMXY, (c) AN, and (d) 2,6-XY in CH (solid line) and MeCN (broken line).

The absorption and fluorescence spectra of AN and alkylated ANs in acidic aqueous solution at 298 K are shown in Fig. 2. The ground-state pK_a values of these compounds are reported to be 3.9–5.1 as shown in Table 1. Hence the absorption spectra exhibited in Fig. 2 are attributable to the protonated forms ($ANsH^+$) of each alkylated AN. This can be confirmed by their spectral shapes resembling the corresponding toluene derivatives. Table 1 shows that the first absorption bands of protonated AN derivatives are ca. $1000\,cm^{-1}$ red-shifted by alkylation (see $\tilde{\nu}^H_{max}$(abs) in Table 1), which would be due to an electronic effect of the substituents. The corresponding neutral compounds except for 4-TL give almost the same peak wavelengths for the first absorption band with that of AN (see $\tilde{\nu}^N_{max}$(abs)). The fluorescence spectra of AN, 4-TL, 2-TL and 2-EAN are ascribed mainly to the deprotonated forms (ANs). Since the excitation spectra monitored at the fluorescence maxima coincided well with the absorption spectrum of the protonated form, the proton-dissociation is found to take place in the excited singlet state. In the fluorescence spectra of 2,6-XY and 2,6-DEAN, dual fluorescence due to the protonated and deprotonated forms are seen, suggesting their

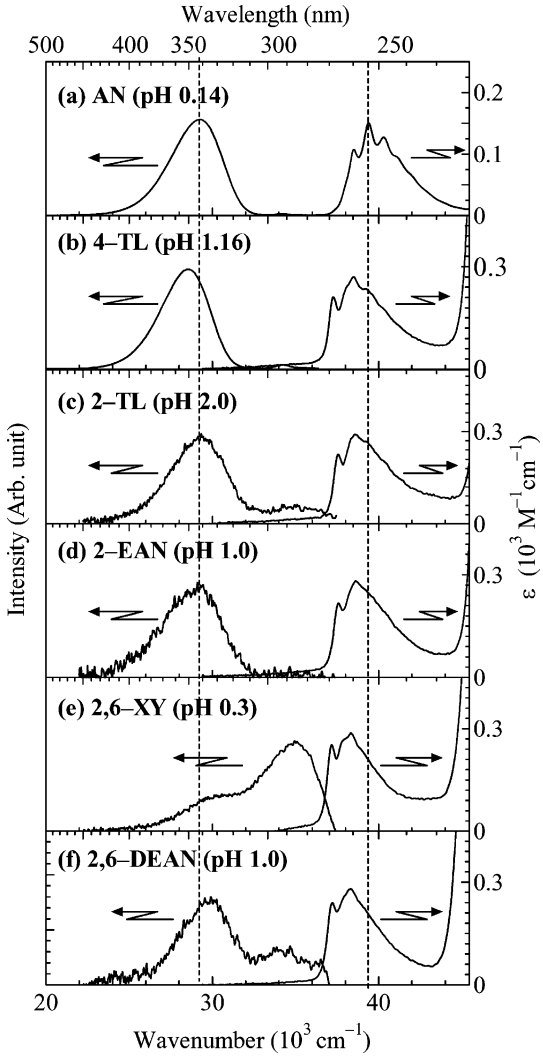

Fig. 2. Absorption and fluorescence spectra of (a) AN at pH 0.14, (b) 4-TL at pH 1.16, (c) 2-TL at pH 2.0, (d) 2-EAN at pH 1.0, (e) 2,6-XY at pH 0.3, and (f) 2,6-DEAN at pH 1.0 in aqueous solution.

slower proton-dissociation rates compared to those of the other compounds.

The absorption and fluorescence maxima of the deprotonated and protonated forms are listed in Table 1 together with their Stokes shifts. The Stokes shift between the absorption maximum of the protonated form and the fluorescence maximum of the deprotonated form ($\Delta\tilde{\nu}^{HN}$) of each compound is also shown in Table 1, which tends to decrease with alkylation at the *ortho* position.

3.2. Fluorescence time profiles

Fig. 3 shows the fluorescence time profiles of AN and its derivatives monitored at peak wavelengths of the emission from the deprotonated species. Each time profile shows rise and decay components, indicating that proton dissociation takes place upon electronic excitation. In order to analyze these fluorescence time profiles, we measured the fluorescence lifetime of the neutral AN derivatives (deprotonated species) at pH > 6.0. The fluorescence decay signals of ANs could be fitted to single exponential decay and the rate constants obtained are listed in Table 2. Interestingly the fluorescence lifetimes of these compounds in water are decreased significantly compared with those in organic solvents [52], showing that strong fluorescence quenching is involved in water. It should also be noted here that the water-induced quenching is enhanced remarkably by alkyl substitution at the *ortho* position of AN. Similar fluorescence quenching due to the presence of solvent water has also been recognized for other aromatic amines [53–56]. The significant fluorescence quenching in *ortho* alkylated ANs suggests that hydrophobic hydration around the amino group due to the presence of the alkyl group is related to the fluorescence quenching. One possible explanation would be that the hydrogen-bonding interactions between the N–H moiety of the amino group and structured water induce efficient nonradiative processes. The study of the fluorescence quenching of AN derivatives due to the presence of water is now in progress.

Under moderately acidic conditions (pH > 1.0), contribution of the proton recombination ($k_{rec}[H_3O^+]$ in Scheme 1) would be negligible. Therefore, the fluorescence time profiles shown in Fig. 3 can be represented by consecutive reaction kinetics: in the compounds which give very short fluorescence lifetime for the deprotonated form (2-TL, 2-EAN, 2,6-XY and 2,6-DEAN), the rise and decay

Table 1
pK_a values in the ground state, absorption ($\tilde{\nu}^{H}_{max}$(abs)) and fluorescence maxima ($\tilde{\nu}^{H}_{max}$(flu)) of ANsH$^+$, absorption ($\tilde{\nu}^{N}_{max}$(abs)) and fluorescence ($\tilde{\nu}^{N}_{max}$(flu)) maxima of ANs, Stokes shifts of ANsH$^+$ ($\Delta\tilde{\nu}^{H}$) and ANs ($\Delta\tilde{\nu}^{N}$) and enthalpy change (ΔH) of ground-state proton-dissociation reaction

Compound	pK_a[a]	ΔH (kJ mol^{-1})	$\tilde{\nu}^{H}_{max}$(abs) (cm^{-1})	$\tilde{\nu}^{H}_{max}$(flu) (cm^{-1})	($\Delta\tilde{\nu}^{H}$) (cm^{-1})[b]	$\tilde{\nu}^{N}_{max}$(abs) (cm^{-1})	$\tilde{\nu}^{N}_{max}$(flu) (cm^{-1})	$\Delta\tilde{\nu}^{N}$ (cm^{-1})[c]	$\Delta\tilde{\nu}^{HN}$ (cm^{-1})[d]
AN	4.6	26	39 400	36 200	3200	35 900	29 100	6800	10 300
4-TL	5.1	29	38 400	35 600	2800	34 800	28 500	6300	9 900
2-TL	4.4	25	38 500	35 600	2900	35 800	29 300	6500	9 200
2-EAN	4.5	26	38 600	34 900	3700	35 600	29 300	6300	9 300
2,6-XY	4.0	23	38 300	35 100	3200	35800	29 700	6100	8 600
2,6-DEAN	3.9	22	38 300	34 300	4000	35 600	29 600	6000	8 700

[a] Form Ref. [51].
[b] $\Delta\tilde{\nu}^{H} = \nu^{H}_{max}(abs) - \tilde{\nu}^{H}_{max}(flu)$.
[c] $\Delta\tilde{\nu}^{N} = \nu^{N}_{max}(abs) - \tilde{\nu}^{N}_{max}(flu)$.
[d] $\Delta\tilde{\nu}^{HN} = \nu^{H}_{max}(abs) - \tilde{\nu}^{N}_{max}(flu)$.

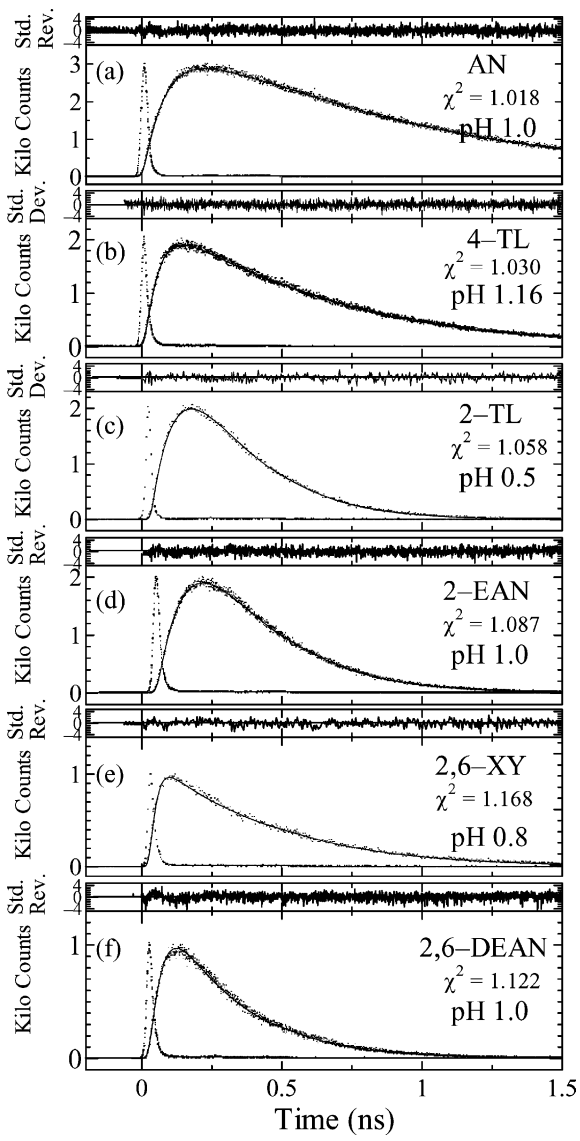

Fig. 3. Time profiles of ^{1}ANs* fluorescence monitored at 340 nm upon electronic excitation of ANsH$^+$: (a) AN at pH 1.0; (b) 4-TL at pH 1.16; (c) 2-TL at pH 0.5; (d) 2-EAN at pH 1.0; (e) 2,6-XY at pH 0.8; (f) 2,6-DEAN at pH 1.0, in aqueous solution. The solid line is the best fit of the experimental data to a biexponential decay law.

components in Fig. 3 correspond approximately to the decay rates of ^{1}ANs* ($k_0' + k_q'[H_3O^+]$) and ^{1}ANsH^{+*} ($k_0 + k_{dis}$), respectively (see Scheme 1).

3.3. Proton-dissociation rate

To determine the k_{dis} values for the proton-dissociation reaction of ^{1}ANsH^{+*}, picosecond time-resolved fluorescence measurements were carried out at $[H_3O^+]$ = 0.01–0.5 M in aqueous solution. The rate equations for the concentration of the S_1 state of neutral AN derivatives (^{1}ANs*) and their protonated ions (^{1}ANsH^{+*}) can be written as

$$\frac{d[^1ANsH^{+*}]}{dt} = -(k_0 + k_{dis})[^1ANsH^{+*}] + k_{rec}[H_3O^+][^1ANs^*] \quad (2)$$

$$\frac{d[^1ANs^*]}{dt} = -\{k_0' + (k_{rec} + k_q')[H_3O^+]\}[^1ANs^*] + k_{dis}[^1ANsH^{+*}] \quad (3)$$

By solving Eqs. (2) and (3), the time-dependent concentration of $[^1ANs^*]$ is obtained as

$$[^1ANs^*] = \frac{[^1ANsH^{+*}]_0 k_{dis}}{\lambda_2 - \lambda_1}\{\exp(-\lambda_1 t) - \exp(-\lambda_2 t)\} \quad (4)$$

where

$$\lambda_{1,2} = \tfrac{1}{2}[(a + a') \mp \{(a - a')^2 + 4k_{dis}k_{rec}[H_3O^+]\}^{1/2}]$$

and $[^1ANsH^{+*}]_0$ is the initial concentration of the protonated AN derivatives in the excited singlet state. The parameters a and a' are defined as

$$a = k_0 + k_{dis} \quad (5)$$

$$a' = k_0' + (k_{rec} + k_q')[H_3O^+] \quad (6)$$

The λ_1 and λ_2 values in Eq. (4) were determined by deconvolution analyses of the fluorescence time profile of ^{1}ANs*. The quantity $(\lambda_1 + \lambda_2)$ was plotted as a function of $[H_3O^+]$ according to the following relation:

$$\lambda_1 + \lambda_2 = (k_0 + k_0' + k_{dis}) + (k_{rec} + k_q')[H_3O^+] \quad (7)$$

The results for 2-EAN at different temperatures are shown in Fig. 4. From the slope and intercept of the straight lines in Fig. 4, the $(k_{rec} + k_q')$ and $(k_0 + k_0' + k_{dis})$ values at 298 K can be obtained as 3.0×10^9 M^{-1} s^{-1} and 1.5×10^{10} s^{-1} for 2-EAN. The rate parameters for ANs obtained at 298 K are shown in Table 2. For aqueous 2-EAN, the $(k_{rec} + k_q')$ values are found to be $\sim 10^9$ M^{-1} s^{-1} in the temperature range of 278–313 K, which are much smaller than the diffusion-controlled rate (5×10^{10} M^{-1} s^{-1}) [57] estimated for bimolecular reactions involving the hydronium ion (H_{aq}^+) in aqueous solution. The slow recombination rate ($\leq 10^9$ M^{-1} s^{-1}) for the reaction between ^{1}ANs* and H_{aq}^+ is in marked contrast with the almost diffusion-controlled rate (5.8×10^{10} M^{-1} s^{-1} at 298 K) [14] for the recombination reaction between excited 1-naphtholate anion and H_{aq}^+. In the latter case Coulombic interactions are found to play an important role in the geminate recombination reaction. In the *N*-alkylated ANs, the magnitude of $(k_{rec} + k_q')$ tends to become larger than that of AN, probably due to enhancement in the rate constant of proton-induced quenching (k_q').

Since the k_0 and k_0' values can be determined by fluorescence lifetime measurements, k_{dis} can be obtained by subtracting $(k_0 + k_0')$ from the value of the intercept, as listed in Table 2. It should be noted here that alkylation at

Table 2
Intrinsic decay rate constants of ^{1}ANsH^{+*} (k_0) and ^{1}ANs* (k_0'), k_{rec} and k_q, and proton-dissociation rate constant (k_{dis}) at 298 K, and activation energy (E_a), frequency factor (A), and reaction enthalpy (ΔH^*) of proton dissociation of ^{1}ANsH^{+*}

Compound	k_0 ($\times 10^9$ s^{-1})	(k_0') ($\times 10^9$ s^{-1})	$k_{rec}+k_q$ ($\times 10^9$ s^{-1})	k_{dis} ($\times 10^9$ s^{-1})	E_a (kJ mol^{-1})	A ($\times 10^{12}$ s^{-1})	ΔH^* (kJ mol^{-1})[a]
AN	0.65	1.1	<0.1	14	11	1.0	−37
4-TL	1.9	1.4	1.8	20	8.5	0.6	−35
2-TL	1.1	8.9	0.7	4.1	11	0.4	−29
2-EAN	1.3	6	3.0	7.3	12	0.9	−26
2,6-XY	1.1	40		1.7[b]	17	1.3	−24
2,6-DEAN	1.9	21		2.7[b]	14	0.1	−22

[a] Estimated by the energy relationships shown in Scheme 3.
[b] Estimated by subtracting k_0 from the decay rate of ^{1}ANs* which corresponds to the decay rate (k_0+k_{dis}) of ^{1}ANsH^{+*} (see text).

the *ortho* position results in a significant decrease of the proton-dissociation rate, while methylation at the 4-position of the aromatic ring enhances the proton-dissociation rate. It can also be recognized that the proton-dissociation rate ($k_{dis} = 1.4 \times 10^{10}$ s^{-1}) for AN at 298 K is much faster than those for the other aromatic amines reported so far, e.g. k_{dis} of 1-naphthylamine in H_2O–CH_3CN (95:5, v/v) [34] and 1-aminopyrene in H_2O–CH_3CN (1:1, v/v) [35] have been reported as 1.3×10^9 and 1.8×10^9 s^{-1}, respectively. The dielectric relaxation time of water has been reported as $\tau_1 = 8.4$ ps and $\tau_2 = 1.1$ ps at 298 K [58]. Although the large k_{dis} value (1.4×10^{10} s^{-1}) is seen for AN, the proton-transfer rate is found to be much slower than the solvent relaxation time of water. Interestingly, the proton-dissociation rate of AN in D_2O ($k_{dis} = 2.5 \times 10^9$ s^{-1}) was much slower than that in H_2O ($k_{dis} = 1.4 \times 10^{10}$ s^{-1}), suggesting a significant role of tunneling in the reaction.

3.4. Effect of ortho alkyl group on the proton-dissociation

In order to reveal the effect of *ortho* substituent on the proton dissociation, we measured the activation energy for the proton-dissociation reaction from ^{1}ANsH^{+*}. Fig. 5 shows the Arrhenius plot for the k_{dis} value of ^{1}ANsH^{+*}. From the slope and intercept of the straight lines in Fig. 5 the activation energy (E_a) and frequency factor (A) were obtained as shown in Table 2. The activation energies of AN and monoalkylated ANs are about 10 kJ mol^{-1}, which is almost the same with the activation energy for the proton mobility in water (10 kJ mol^{-1}) [26]. The observed activation energy is attributed to the energy required for rearrangement of the hydrogen bonding in the normal water structure to accept a proton. The activation energies for 2,6-XY and 2,6-DEAN are larger than those of the other compounds in Table 2. This indicates that the presence of the *ortho* alkyl groups inhibits reorganization of water molecules near the amino group and decreases the proton-dissociation rate. The frequency factors were obtained to be 10^{11}–10^{12} s^{-1}, which are about two orders of magnitude larger than that of 2-naphthol [10].

The reaction enthalpy (ΔH^*) for the proton dissociation in the excited state can be evaluated from the pK_a value in the ground state and spectral properties of protonated and deprotonated forms. Scheme 3 shows the thermochemical relationship for the acid–base reactions of 2-EAN in the ground and excited states, where the energy difference (ΔH_{solv}) between the equilibrium (EQ) and Franck–Condon (FC) state is estimated from the absorption ($\tilde{\nu}_{max}$(abs)) and fluorescence ($\tilde{\nu}_{max}$(flu)) maxima as $\tilde{\nu}_{max}(abs) - \tilde{\nu}_{max}(flu) = 2\Delta H_{solv}$. One can see clearly from Scheme 3 that the proton dissociation of 2-EAN in the S_1 state is an exothermic reaction.

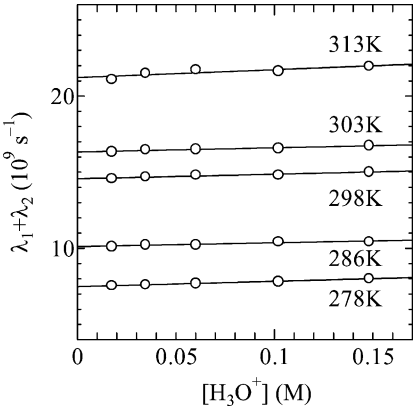

Fig. 4. Plots of ($\lambda_1 + \lambda_2$) as a function of [H_3O^+] for 2-EAN at 278, 286, 198, 303, and 313 K.

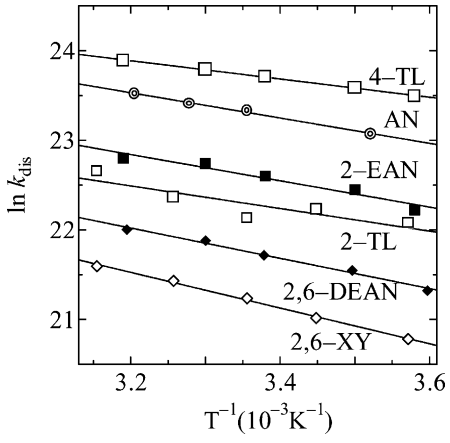

Fig. 5. Arrhenius plots for the proton-dissociation rate constant (k_{dis}) of ^{1}ANsH^{+*} in aqueous solution.

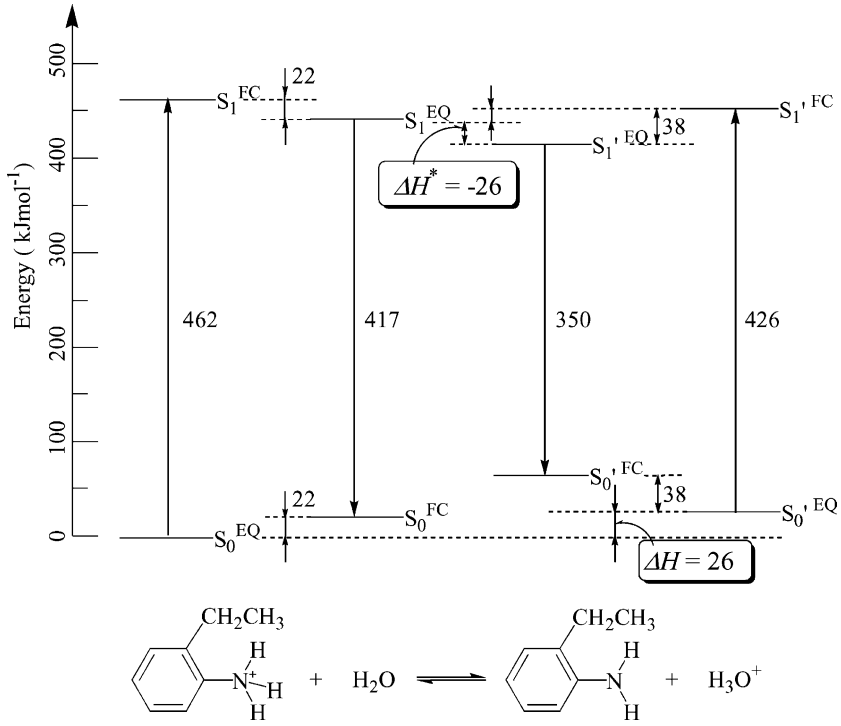

Scheme 3. Thermochemical energy diagram for the proton-dissociation reaction of 2-EAN in the ground and excited states.

The estimated ΔH^* value for each compound is listed in Table 2. It can be seen from Table 2 that the reaction exothermicity for the proton dissociation tends to decrease with alkyl substitution at the *ortho* position. The relationship between k_{dis} and ΔH^* is depicted in Fig. 6. Comparing k_{dis} of 4-TL and those of the other compounds, the *ortho* substituent is found to decrease the proton-dissociation rate more remarkably than expected from exothermicity of the reaction, i.e. the substituent effect of the *ortho* alkyl group on proton dissociation cannot be explained by only electronic effect (electron-donating character).

Robinson and coworkers [10] measured the deprotonation rate in the excited singlet state of 1- and 2-naphthols in various water–ethanol mixtures. From analyses of the experimental results based on the Markov random walk method, the water cluster $(H_2O)_{4\pm1}$ was identified as the effective proton acceptor for the proton dissociation. Tolbert et al. [59] studied the excited-state proton-transfer reactions of 1-propyl-2-naphthol, 1-(3-hydroxypropyl)-2-naphthol and 1-(2,3-dihydroxypropyl)-2-naphthol in aqueous methanol solutions. They found that the presence of one or more hydroxy groups on an alkyl side chain incorporated into the photoacid facilitates the proton transfer to water in methanol solution. The results were compatible with a model in which a proton is transferred to a single water molecule, forming a hydronium ion solvated both intra- and intermolecularly by alcohol moieties. The study of Tolbert et al. also showed the importance of local water structure near the amino group in proton transfer to solvent water. One possible explanation for the reduction of the proton-dissociation rate in *o*-alkylated ANs is based on the hydrophobic hydration around the alkyl group. In the vicinity of the amino group the hydrophobic alkyl group(s) would act as structure-making group for water. As a result, the orientational relaxation of water molecules suitable for the proton transfer would be depressed in the alkylated ANs.

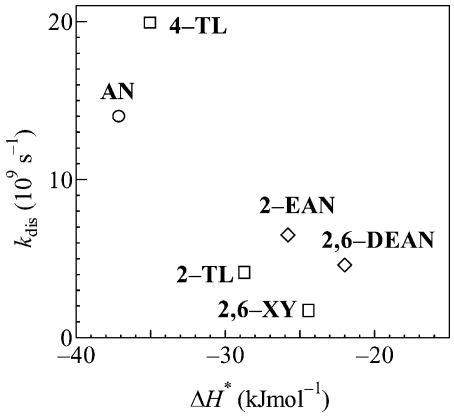

Fig. 6. Plots of k_{dis} for $^1ANsH^{+*}$ as a function of reaction enthalpy (ΔH^*) for the excited-state proton transfer to solvent.

Acknowledgements

This work was supported by Grants-in-Aid (No. 14540465) from the Ministry of Education, Culture, Sports, and Science, and Technology of Japan.

References

[1] L.M. Tolbert, K.M. Solntsev, Acc. Chem. Res. 35 (2002) 19.
[2] A.K. Mishra, in: Ramamurthy, K.S. Schanze (Eds.), Molecular and Supramolecular Photochemistry Series, vol. 8, Marcel Dekker, New York, 2001, Chapter 10, pp. 577.
[3] T. Elsaesser, in: J. Manz, L. Woste (Eds.), Femtosecond Chemistry, VCH, Weinheim, 1995, Chapter 18.
[4] L.G. Arnaut, S.J. Formosinho, J. Photochem. Photobiol. A 75 (1993) 1.
[5] S.J. Formosinho, L.G. Arnaut, J. Photochem. Photobiol. A 75 (1993) 21.
[6] E.M. Kosower, D. Huppert, Annu. Rev. Phys. Chem. 37 (1986) 127.
[7] G.W. Robinson, P.J. Thistlethwaite, J. Lee, J. Phys. Chem. 90 (1986) 4224.
[8] H. Shizuka, Acc. Chem. Res. 18 (1985) 141.
[9] K. Tsutsumi, H. Shizuka, Z. Phys. Chem. 122 (1980) 129.
[10] J. Lee, R.D. Griffin, G.W. Robinson, J. Chem. Phys. 82 (1985) 4920.
[11] J. Lee, G.W. Robinson, S.P. Webb, L.A. Philips, J.H. Clark, J. Am. Chem. Soc. 108 (1986) 6538.
[12] S.P. Webb, L.A. Philips, S.W. Yeh, L.M. Tolbert, J.H. Clark, J. Phys. Chem. 90 (1986) 5154.
[13] G.W. Robinson, P.J. Thistlethwaite, J. Lee, J. Phys. Chem. 90 (1986) 4920.
[14] J. Lee, G.W. Robinson, M.-P. Bassez, J. Am. Chem. Soc. 108 (1986) 7477.
[15] J. Lee, J. Am. Chem. Soc. 111 (1989) 427.
[16] R. Krishnan, T.G. Fillingim, J. Lee, G.W. Robinson, J. Am. Chem. Soc. 112 (1990) 1353.
[17] R. Krishnan, J. Lee, G.W. Robinson, J. Phys. Chem. 94 (1990) 6365.
[18] E. Pines, D. Huppert, N. Agmon, J. Chem. Phys. 88 (1988) 5620.
[19] N. Agmon, E. Pines, D. Huppert, J. Chem. Phys. 88 (1988) 5631.
[20] N. Agmon, D. Huppert, A. Masad, E. Pines, J. Phys. Chem. 95 (1991) 10407.
[21] B. Cohen, D. Huppert, J. Phys. Chem. A 104 (2000) 2663.
[22] B. Cohen, D. Huppert, J. Phys. Chem. A 105 (2001) 2980.
[23] L.M. Tolbert, J.E. Haubrich, J. Am. Chem. Soc. 116 (1994) 10593.
[24] D. Huppert, L.M. Tolbert, S. Linares-Samaniego, J. Phys. Chem. A 101 (1997) 4602.
[25] K.M. Solntsev, D. Huppert, N. Agmon, J. Phys. Chem. A 103 (1999) 6984.
[26] K.M. Solntsev, D. Huppert, N. Agmon, L.M. Tolbert, J. Phys. Chem. A 104 (2000) 4658.
[27] A. Suwaiyan, F. Al-Adel, A. Hamdan, U.K.A. Klein, J. Phys. Chem. 94 (1990) 7423.
[28] M.T. Htun, A. Suwaiyan, U.K.A. Klein, Chem. Phys. Lett. 243 (1995) 506.
[29] M.T. Htun, A. Suwaiyan, U.K.A. Klein, Chem. Phys. Lett. 243 (1995) 512.
[30] R. Knochenmuss, S. Leutwyler, J. Chem. Phys. 91 (1989) 1268.
[31] R. Knochenmuss, I. Fischer, D. Lührs, Q. Lin, Isr. J. Chem. 39 (1999) 221.
[32] S.K. Kim, J.J. Breen, D.M. Willberg, L.W. Peng, A. Heikal, J.A. Syage, A.H. Zewail, J. Phys. Chem. 99 (1995) 7421.
[33] J.A. Syage, J. Phys. Chem. 99 (1995) 5772.
[34] K. Tsutsumi, H. Shizuka, Z. Phys. Chem. N.F. 111 (1978) 129.
[35] H. Shizuka, K. Tsutsumi, H. Takeuchi, I. Tanaka, Chem. Phys. 59 (1981) 183.
[36] K. Tsutsumi, S. Sekiguchi, H. Shizuka, J. Chem. Soc., Faraday Trans. 1 78 (1982) 1087.
[37] S. Tajima, S. Tobita, H. Shizuka, J. Phys. Chem. A 104 (2000) 11270.
[38] E. Pines, G.R. Fleming, J. Phys. Chem. 95 (1991) 10448.
[39] J.E. Hansen, E. Pines, G.R. Fleming, J. Phys. Chem. 96 (1992) 6904.
[40] J.C. Joshi, D.D. Pant, Chem. Phys. Lett. 59 (1978) 529.
[41] N. Agmon, J. Chem. Phys. 110 (1999) 2175.
[42] E.L. Wehry, L.B. Rogers, J. Am. Chem. Soc. 87 (1965) 4234.
[43] S.G. Schulman, W.R. Vincent, W.J.M. Underberg, J. Phys. Chem. 85 (1981) 4068.
[44] K.C. Gross, P.G. Seybold, Int. J. Quant. Chem. 80 (2000) 1107.
[45] T. Yoshihara, H. Shimada, H. Shizuka, S. Tobita, Phys. Chem. Chem. Phys. 3 (2001) 4972.
[46] M.J. Frisch, G.W. Trucks, H.B. Schlegel, G.E. Scuseria, M.A. Robb, J.R. Cheeseman, V.G. Zakrzewski, J.A. Montgomery Jr., R.E. Stratmann, J.C. Burant, S. Dapprich, J.M. Millam, A.D. Daniels, K.N. Kudin, M.C. Strain, O. Farkas, J. Tomasi, V. Barone, M. Cossi, R. Cammi, B. Mennucci, C. Pomelli, C. Adamo, S. Clifford, J. Ochterski, G.A. Petersson, P.Y. Ayala, Q. Cui, K. Morokuma, D.K. Malick, A.D. Rabuck, K. Raghavachari, J.B. Foresman, J. Cioslowski, J.V. Ortiz, A.G. Baboul, B.B. Stefanov, G. Liu, A. Liashenko, P. Piskorz, I. Komaromi, R. Gomperts, R.L. Martin, D.J. Fox, T. Keith, M.A. Al-Laham, C.Y. Peng, A. Nanayakkara, M. Challacombe, P.M.W. Gill, B. Johnson, W. Chen, M.W. Wong, J.L. Andres, C. Gonzalez, M. Head-Gordon, E.S. Replogle, J.A. Pople, Gaussian 98, Gaussian, Inc., Pittsburgh, PA, 1998.
[47] K. Suzuki, H. Tanabe, S. Tobita, H. Shizuka, J. Phys. Chem. A 101 (1997) 4496.
[48] I. Rückert, A. Demeter, O. Morawski, W. Kühnle, E. Tauer, K.A. Zachariasse, J. Phys. Chem. A 103 (1999) 1958.
[49] K. Suzuki, A. Demeter, W. Kuhnle, E. Tauer, K.A. Zachariasse, S. Tobita, H. Shizuka, Phys. Chem. Chem. Phys. 2 (2000) 981.
[50] S. Tobita, R. Kamiyama, K. Takehira, T. Yoshihara, S. Yotoriyama, H. Shizuka, Anal. Sci. 17 (2001) 50.
[51] A.J. Dean, Lange's Handbook of Chemistry, McGraw-Hill, New York, 1973.
[52] S. Tobita, K. Ida, S. Shiobara, Res. Chem. Intermed. 27 (2001) 205.
[53] D. Yuan, R.G. Brown, J. Phys. Chem. A 101 (1997) 3461.
[54] R.J. Visser, P.C.M. Weisenborn, J. Konijnenbeerg, B.H. Huizer, C.A.G.O. Varma, J. Photochem. 32 (1986) 217.
[55] J. Lee, G.W. Robinson, J. Am. Chem. Soc. 107 (1985) 6153.
[56] P.J. Sadkowski, G.R. Fleming, Chem. Phys. 54 (1980) 79.
[57] S. Tajima, S. Tobita, H. Shizuka, J. Phys. Chem. A 103 (1999) 6097.
[58] R. Buchner, J. Barthel, J. Stauber, Chem. Phys. Lett. 306 (1999) 57.
[59] L.M. Tolbert, L.C. Harvey, R.C. Lum, J. Phys. Chem. 97 (1993) 13335.